
SINDY-KANs: SPARSE IDENTIFICATION OF NON-LINEAR DYNAMICS THROUGH KOLMOGOROV-ARNOLD NETWORKS

A PREPRINT

 **Amanda A. Howard**
Pacific Northwest National Laboratory
Richland, WA 99354
amanda.howard@pnnl.gov

 **Nicholas Zolman**
University of Washington
Seattle, WA 98195
nzolman@uw.edu

 **Bruno Jacob**
Pacific Northwest National Laboratory
Richland, WA 99354
bruno.jacob@pnnl.gov

 **Steven L. Brunton**
University of Washington
Seattle, WA 98195
sbrunton@uw.edu

 **Panos Stinis**
Pacific Northwest National Laboratory
Richland, WA 99354
panagiotis.stinis@pnnl.gov

ABSTRACT

Kolmogorov-Arnold networks (KANs) have arisen as a potential way to enhance the interpretability of machine learning. However, solutions learned by KANs are not necessarily interpretable, in the sense of being sparse or parsimonious. Sparse identification of nonlinear dynamics (SINDy) is a complementary approach that allows for learning sparse equations for dynamical systems from data; however, learned equations are limited by the library. In this work, we present SINDy-KANs, which simultaneously train a KAN and a SINDy-like representation to increase interpretability of KAN representations with SINDy applied at the level of each activation function, while maintaining the function compositions possible through deep KANs. We apply our method to a number of symbolic regression tasks, including dynamical systems, to show accurate equation discovery across a range of systems.

Keywords Kolmogorov-Arnold networks · SINDy · Symbolic regression

1 Introduction

Kolmogorov-Arnold networks (KANs), which use the Kolmogorov-Arnold Theorem as inspiration, have recently been developed as an alternative to multilayer perceptrons (MLPs) [1, 2]. Unlike MLPs, which use fixed activation functions with trainable weights, KANs use trainable activation functions. This capability has been promoted as a way to develop interpretable machine learning models, by identifying the trained activation functions. Many variations of KANs have quickly become popular; e.g. physics-informed KANs (PIKANs) [3, 4, 5, 6], graph KANs [7, 8, 9], and deep operator KANs [10]. For physics-informed training in [3], modifications of KANs can have similar accuracy to physics-informed neural networks [11]. KANs have been applied to a wide variety of problems, including satellite image classification [12], time-series analysis [13], and fluid dynamics [14, 15, 16]. For a summary of advances in training KANs, we refer the reader to recent surveys, including [17, 18, 19].

Much of the previous literature has applied KANs in a way similar to an MLP, without identifying or analyzing the functions through symbolic regression. Many papers discussing interpretability of KANs, such as [20], qualitatively analyze the learned activation functions, but do not connect them to a learned equation. When symbolic regression is performed with KANs, the learned equations are often quite complex, making interpretability difficult (although still certainly easier than weights and biases learned with MLPs, as noted by [21]). Significant pruning of the KAN during training before the symbolic regression has also been applied to reduce spurious terms in the learned equations, such as in [22]. Nevertheless, symbolic regression has been successful with KANs—such as for radio map predictions [23], for predicting the pressure and flow rate of flexible electrohydrodynamic pumps [24], and even providing interpretable

predictions of cancer development [25]. However, these approaches can be limited; e.g., [25] only used a network with a single layer, so no interaction between the variables is possible beyond a linear combination. In [26], the authors performed symbolic regression for reservoir water temperatures, progressively increasing the number of input variables. When the number of variables was large the accuracy improved through nested nonlinearities, but this reduced the interpretability of the model. Recent work has extended the symbolic regression functionality of KANs by using a large language model to identify the target functions [27]. In a different approach, [28] improved symbolic regression with KANs by breaking the problem into smaller decompositions, which allows for iteratively training shallower (single layer) KANs.

One issue with symbolic regression with KANs is that in [1], the activation functions are identified by comparing with a library of candidate functions. As noted in [29], the learned activation functions will not necessarily align with the candidate functions, even if it is known that the candidate functions can be composed to output the target function. This limits the applicability of symbolic regression as implemented in [1], and necessitates work that causes the activation functions to necessarily align with the candidate functions. For example, [29] uses a dictionary of symbolic and dense terms as the candidate function, with learnable gates that sparsify the representation. Here, we aim to make symbolic regression performed with KANs more interpretable by directly learning compositions of sparse equation representations through a SINDy-like approach.

The sparse identification of nonlinear dynamics (SINDy) framework [30] is a widely adopted method for identifying sparse, interpretable models of dynamical systems from data. SINDy has been widely applied, including turbulence modeling [31, 32], network modeling [33], and model predictive control [34], and has been extended for reinforcement learning [35], extremely noisy data [36, 37, 38, 39, 40], and nonlinear dynamical systems [41], among many other extensions. One extension most similar to this work is ADAM-SINDy [42], where the SINDy coefficients are determined by the ADAM optimizer [43]. Compared with standard SINDy, ADAM-SINDy allows for parameterized libraries, enabling more customization for the candidate functions.

In this work we present SINDy-KANs, which combine the sparse function identification of SINDy with the deep learning of KANs. Through KAN layers, SINDy-KANs allow for symbolic regression of function compositions not possible with SINDy. Additionally, SINDy-KANs enforce learning parsimonious, interpretable equations more directly than standard KANs. In a sense, SINDy-KANs can be thought of as a deep version of ADAM-SINDy [42], where the SINDy coefficients are directly learned. Both SINDy and KANs at the basic level learn basis function expansions, so combining the methods is especially harmonious. We present the methodology behind SINDy-KANs in Secs. 2 and 3 and a series of experiments for both discovery of equations and dynamical systems from data in Sec. 4.

2 Background methodology

2.1 Kolmogorov-Arnold networks

Kolmogorov-Arnold networks (KANs) [1] approximate a multivariate function $f(\mathbf{x})$ by composition and addition of univariate functions. We consider a KAN with L layers and $\{n_j\}_{j=0}^L$ nodes per layer (denoted $[n_0, n_1, \dots, n_L]$). We denote the activation function that connects the (ℓ, i) and $(\ell + 1, j)$ nodes by $\varphi_{\ell,j,i}$. Each KAN layer takes as univariate input $\mathbf{x}^{(\ell)} = \{x_1^{(\ell)}, \dots, x_{n_L}^{(\ell)}\}$. The input to the KAN is $\mathbf{x} = \mathbf{x}^{(0)}$. Then, each KAN layer can be expressed as

$$\mathbf{x}^{(\ell+1)} = \sum_{i=0}^{n_L} \varphi_{\ell,j,i}(x_i^{(\ell)}). \quad (1)$$

We denote the output of the KAN by $\mathcal{K}(\mathbf{x})$. The activation functions are represented (on a grid with g points) by a weighted combination of a basis function $b(x)$ and a B-spline,

$$\varphi(x) = w_b b(x) + w_s \text{spline}(x), \quad (2)$$

where

$$b(x) = \frac{x}{1 + e^{-x}},$$

and

$$\text{spline}(x) = \sum_i c_i B_i(x).$$

Here, $B_i(x)$ is a polynomial of degree k , typically chosen with $k = 3$ or 5 and fixed as $k = 5$ in this work. c_i, w_b , and w_s are trainable parameters if not predetermined by the user. We refer the reader to [1] for details on training KANs.

Data-driven KANs are trained by minimizing the loss function given by the difference between the KAN representation and provided data:

$$\mathcal{L}_{\text{KAN}} = \|f(\mathbf{x}) - \mathcal{K}(\mathbf{x})\|_2^2. \quad (3)$$

While KANs can represent products of the input functions through the sums of quadratics (e.g., $xy = \frac{1}{4}(x+y)^2 - \frac{1}{4}(x-y)^2$), it is simpler and easier to interpret when KANs have multiplication nodes added. Multiple methods have been developed to do so, including MultKANs [2] and LeanKAN [44]. Both of these methods have advantages and disadvantages in terms of accuracy, trainable parameters, and computational complexity. For this work, we introduce multiplication-enabled KANs where some of the sums of activation functions in each layer are replaced by a product of the activation functions. Specifically, for a KAN layer with n_j nodes, we designate n_j^M of the nodes as multiplication nodes, where the input activation functions for that node are multiplied together. This architecture allows for easier discovery of dynamical systems that contain products of the input variables.

2.2 Sparse identification of nonlinear dynamics

Sparse identification of nonlinear dynamics (SINDy) [30] allows for sparse identification of systems of equations governing dynamical systems. We consider a dynamical system of the form

$$\frac{d}{dt}\mathbf{x}(t) = \mathbf{f}(\mathbf{x}(t)) \quad (4)$$

for $\mathbf{x} \in \mathbb{R}^n$. Available data are sampled at times t_1, t_2, \dots, t_m to create two matrices

$$\mathbf{X} = \begin{bmatrix} \mathbf{x}^T(t_1) \\ \mathbf{x}^T(t_2) \\ \vdots \\ \mathbf{x}^T(t_m) \end{bmatrix} = \begin{bmatrix} x_1(t_1) & x_2(t_1) & \cdots & x_n(t_1) \\ x_1(t_2) & x_2(t_2) & \cdots & x_n(t_2) \\ \vdots & \vdots & \ddots & \vdots \\ x_1(t_m) & x_2(t_m) & \cdots & x_n(t_m) \end{bmatrix} \quad (5)$$

and

$$\dot{\mathbf{X}} = \begin{bmatrix} \dot{\mathbf{x}}^T(t_1) \\ \dot{\mathbf{x}}^T(t_2) \\ \vdots \\ \dot{\mathbf{x}}^T(t_m) \end{bmatrix} = \begin{bmatrix} \dot{x}_1(t_1) & \dot{x}_2(t_1) & \cdots & \dot{x}_n(t_1) \\ \dot{x}_1(t_2) & \dot{x}_2(t_2) & \cdots & \dot{x}_n(t_2) \\ \vdots & \vdots & \ddots & \vdots \\ \dot{x}_1(t_m) & \dot{x}_2(t_m) & \cdots & \dot{x}_n(t_m) \end{bmatrix}. \quad (6)$$

A library of candidate nonlinear functions is denoted by $\Theta(\mathbf{X})$, where each column of $\Theta(\mathbf{X})$ is given by a candidate function:

$$\Theta(\mathbf{X}) = \begin{bmatrix} | & | & | & \cdots & | & | \\ \mathbf{1} & \mathbf{X} & \mathbf{X}^{P_2} & \cdots & \sin(\mathbf{X}) & \cos(\mathbf{X}) \\ | & | & | & & | & | \end{bmatrix}, \quad (7)$$

where \mathbf{X}^{P_2} denotes the quadratic nonlinearities in the state variable \mathbf{x} .

The goal of SINDy is to solve a sparse regression problem for vectors of coefficients $\Xi = [\xi_1 \xi_2 \cdots \xi_n]$ given by

$$\dot{\mathbf{X}} = \Theta(\mathbf{X})\Xi. \quad (8)$$

In practice, obtaining sparse coefficients Ξ is achieved by minimizing the SINDy loss function

$$\mathcal{L}_{\text{SINDy}} = \|\dot{\mathbf{X}} - \Theta(\mathbf{X})\Xi\| + \|\Xi\|_0, \quad (9)$$

where $\|\cdot\|_0$ counts the number of nonzero entries. This non-convex optimization problem is typically solved using sequentially-thresholded least squares regression, which also makes it possible to enforce known symmetries and other physical constraints on the model coefficients [45].

While SINDy and its variants have been very effectively applied to a wide range of applications [46, 47, 48, 49, 50, 51, 52, 53, 54, 31, 32], a disadvantage is that the candidate functions must be determined by the user. If the dynamical system consists of complex functions, such as compositions of functions, determining the proper library of candidate functions can be difficult and/or result in a very large library.

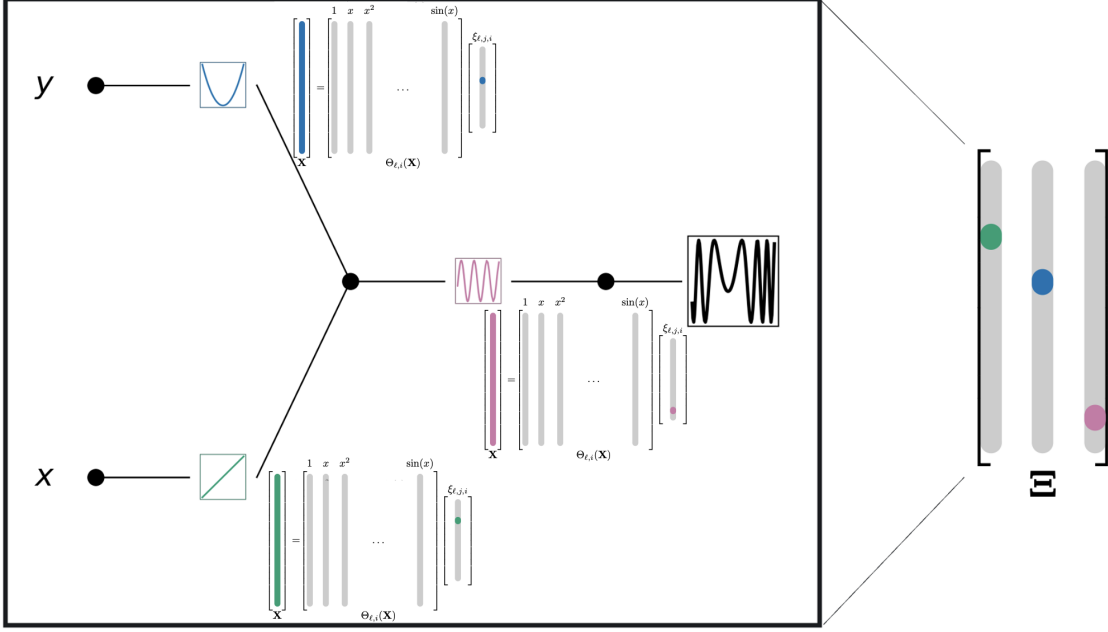


Figure 1: Pictorial representation of a SINDy-KAN for a function $f(x, y) = \sin(x + y^2)$. Each KAN activation function has an associated least squares regression as given in Eq. 13. The learned coefficients are then combined in Ξ .

3 SINDy-KANs

In SINDy-KANs, we perform a SINDy-like sparse regression at each KAN activation function as the system is training. In particular, consider an activation function $\varphi_{\ell,j,i}$ with input $\mathbf{x}_i^{(\ell)}$. We assume available data are sampled at times t_1, t_2, \dots, t_m to create the matrices:

$$\mathbf{X}_i^{(\ell)} = [x_i^{(\ell)}(t_1), x_i^{(\ell)}(t_2), \dots, x_i^{(\ell)}(t_m)]. \quad (10)$$

We construct a library of candidate functions

$$\Theta_{\ell,i}(\mathbf{X}_i^{(\ell)}) = \left[\begin{array}{c|c|c|c|c|c} | & | & | & | & | & | \\ \mathbf{1} & \mathbf{X}_i^{(\ell)} & \mathbf{X}_i^{(\ell)P_2} & \dots & \sin(\mathbf{X}_i^{(\ell)}) & \cos(\mathbf{X}_i^{(\ell)}) \\ | & | & | & | & | & | \end{array} \right]. \quad (11)$$

We note that since KANs consist of univariate activation functions, $\Theta_{\ell,i}(\mathbf{X}_i^{(\ell)})$ is univariate with respect to the input. We also note that $\Theta_{\ell,i}(\mathbf{X}_i^{(\ell)})$ does not have to be the same for all ℓ . Depending on knowledge of the problem, different hidden layers in the SINDy-KAN can be represented by a different set of candidate functions.

Then, we define a sparse vector of coefficients $\xi_{\ell,j,i}$ and

$$\varphi_{\ell,j,i} = \begin{bmatrix} \varphi_{\ell,j,i}(x_i^{(\ell)}(t_1)) \\ \varphi_{\ell,j,i}(x_i^{(\ell)}(t_2)) \\ \vdots \\ \varphi_{\ell,j,i}(x_i^{(\ell)}(t_m)) \end{bmatrix} \quad (12)$$

such that

$$\varphi_{\ell,j,i} = \Theta_{\ell,i}(\mathbf{X}_i^{(\ell)})\xi_{\ell,j,i}. \quad (13)$$

We denote by $\Xi_S = \{\xi_{1,1,1}, \xi_{1,1,2}, \dots, \xi_{L,j,i}\}$ to be the learned coefficients. Once the coefficients Ξ_S are found, the output of the SINDy-KAN can be determined through evaluating the SINDy-KAN representation. A diagram of a SINDy-KAN is given in Fig. 1. A labeled example of a trained SINDy-KAN is given in Fig. 2.

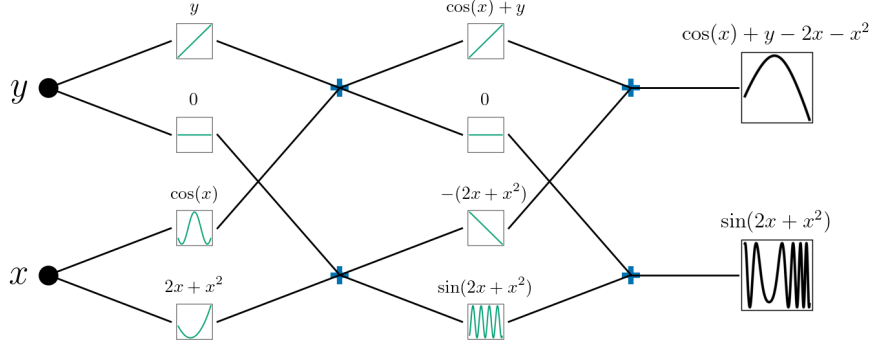


Figure 2: Example of a trained SINDy-KAN for the system of equations $f_1(x, y) = \sin(2x + x^2)$, $f_2(x, y) = \cos(x) + y - 2x - x^2$.

A well-trained SINDy-KAN has a few desirable features. The KAN should agree well with the data (the KAN loss defined in Eq. 3 should be small). Also, the SINDy-KAN representation denoted by $\mathcal{K}_S(\mathbf{x})$ should agree well with the data, giving the error term

$$\mathcal{L}_S = \|\mathbf{f}(\mathbf{x}) - \mathcal{K}_S(\mathbf{x})\|_2^2. \quad (14)$$

The coefficients Ξ_S should be sparse, so $\|\Xi_S\|_1$ is minimized. However, SINDy-KANs are trained using standard neural network optimizers such as ADAM, which struggle with minimizing the L_1 norm of Ξ_S . Instead, we introduce a shadow matrix Λ that consists of trainable entries that represent a sparse version of Ξ_S . Λ is trained to minimize $\lambda\|\Lambda\|_1 + \|\Lambda - \Xi_S\|_2^2$.

We can introduce two additional loss terms. We denote by $\mathcal{K}_\Lambda(\mathbf{x})$ the KAN evaluated with Λ . Then, we can also consider

$$\mathcal{L}_\Lambda = \|\mathbf{f}(\mathbf{x}) - \mathcal{K}_\Lambda(\mathbf{x})\|_2^2. \quad (15)$$

The general SINDy-KAN loss function takes the form:

$$\mathcal{L} = \lambda_{KAN}\mathcal{L}_{KAN} + \lambda_S\mathcal{L}_S + \lambda_\Lambda\mathcal{L}_\Lambda + \lambda_1\|\Lambda\|_1 + \lambda_2\|\Lambda - \Xi_S\|_2^2. \quad (16)$$

Because $\|\Lambda\|_1$ should be $\mathcal{O}(1)$, we note that λ_1 should be on the order of the expected loss \mathcal{L}_S . For the examples in this work we fix $\lambda_{KAN} = 1.0$.

We compare our results with the pykan package, which also does equation discovery as implemented in [1]. In [1], each activation function is restricted to have the form $a + bh(cx + d)$ for scalars a, b, c , and d and a function h found from a given library of functions. In particular, this formulation prevents linear combinations of the library functions, which limits the functions the method can identify. The functions are selected at the end of training, instead of during training, so there is no requirement that the learned activation functions should align with the functions in the library, as noted by [29]. pykan training involves a series of training and sparsification steps that must be managed by the user. In this work, we keep the pykan implementation as close to the implementation in [1] as possible.

SINDy-KANs train a standard KAN and simultaneously find the coefficients $\xi_{\ell,j,i}$ by solving Eq. 13 for each activation function using sparse regression. In other words, SINDy-KANs learn the sparse representation *and* the KAN representation simultaneously. Alternatively, one could train a SINDy-KAN to learn the coefficients $\xi_{\ell,j,i}$ by minimizing Eq. 14. We call this method *direct SINDy-KANs* because the coefficients are learned directly. We discuss direct SINDy-KANs more in Appendix A. While direct SINDy-KANs can accurately train, we find that they are less robust than finding the coefficients $\xi_{\ell,j,i}$ as presented above. They are, however, less expensive to train for large networks, because the computational work at each iteration is significantly lower without solving the sparse regression problems at each KAN node. We leave a further exploration of direct SINDy-KANs for future work.

4 Experiments

We implemented the SINDy-KAN algorithm in jaxKAN [55]. jaxKAN offers several advances in KAN training aimed at increasing accuracy for scientific machine learning including advanced initialization, adaptive grid refinement [56, 57, 58], and additional KAN basis functions [59]. However, in this work we use the B-spline implementation closest to the original KAN formulation in [1] to try and provide direct comparisons with existing literature.

Training parameters for all examples are given in Appendix C in table 4 and table 5.

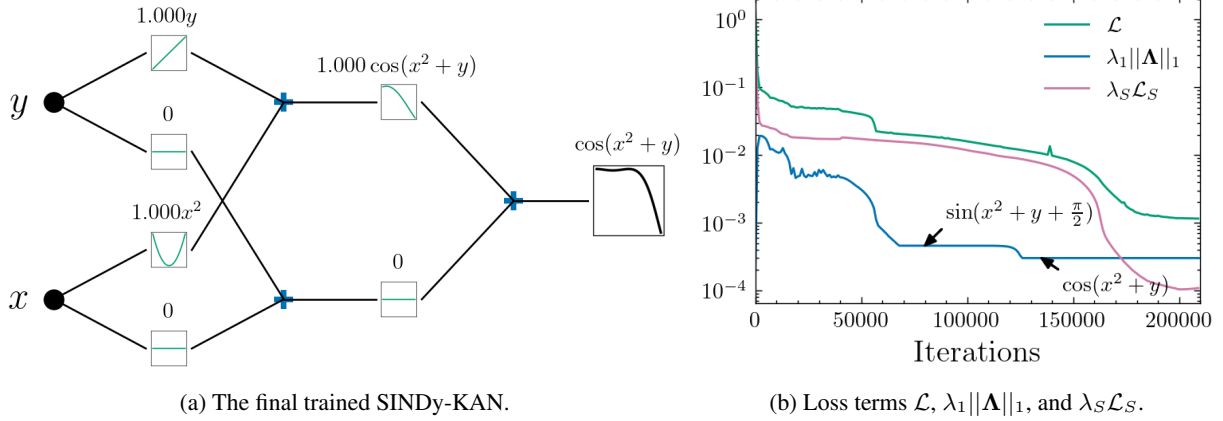


Figure 3: Results for Sec. 4.1. (a) The final trained SINDy-KAN correctly learns the target equation. (b) The loss terms show two plateaus for the L_1 regularization term $\lambda_1 \|\mathbf{A}\|_1$.

4.1 Symbolic regression

In this section we focus on learning symbolic equations directly from data for the equation

$$f(x, y) = \cos(x^2 + y), \quad (17)$$

chosen because it contains a composition of functions (\cos and $x^2 + y$), something that would be difficult to know to include in a typical library of functions for standard SINDy. KANs are able to handle composition by increasing the depth of the network. We take $(x, y) \in [-2.5, 2.5] \times [-2.5, 2.5]$ and use 1,000 randomly selected points as training data. We take the library of candidate functions $\Theta_{\ell, j, i}(\mathbf{x})$ as polynomials up to degree two plus sine and cosine,

$$\Theta_{\ell, i} = \left[\begin{array}{c} | \\ \mathbf{1} \\ | \\ \mathbf{X}_i^{(\ell)} \\ | \\ \mathbf{X}_i^{(\ell)^2} \\ | \\ \sin(\mathbf{X}_i^{(\ell)}) \\ | \\ \cos(\mathbf{X}_i^{(\ell)}) \\ | \end{array} \right]. \quad (18)$$

Hyperparameters used for training are given in Table 4.

The SINDy-KAN learns the correct equation,

$$\mathcal{K}_\Lambda = 0.9999 \cos(1.0000x^2 + 0.9999y),$$

also shown in fig. 3a. `pykan` struggles to learn the composition of functions, resulting in

$$\mathcal{K}^{pykan} = 0.02002x - 0.0275y - 0.5642 \sin(1.7946x - 0.1641y + 3.4794).$$

In particular, `pykan` misses the x^2 term, resulting in larger errors overall.

Examining the loss profiles gives some interesting insight into the SINDy-KAN training. In fig. 3b, we show the total loss \mathcal{L} given by Eq. 16 and the L_1 regularization term $\lambda_1 \|\mathbf{A}\|_1$. After the initial transient training period, $\|\mathbf{A}\|_1$ has two plateaus. Examination of the learned equations at the plateaus shows that the first is at $\|\mathbf{A}\|_1 \approx 3 + \pi/2$, where the SINDy-KAN learns $\sin(x^2 + y + \pi/2)$, which simplifies to the correct equation but is not the sparsest form of the equation. After additional training, the second plateau occurs at $\|\mathbf{A}\|_1 \approx 3$, representing the equation $\cos(x^2 + y)$.

4.2 Differential equation discovery

A common use case for SINDy is identifying dynamical systems of the form given in Eq. 4, where data is given in the form (t, \mathbf{x}) . To use SINDy on this data, it is necessary to take numerical derivatives to find $\frac{d\mathbf{x}}{dt}$. Finding this derivative can be difficult, particularly in the presence of noisy data [30]. Methods used in other work can certainly be used for SINDy-KANs, such finite differences which has successfully applied to SINDy before [30].

4.2.1 Linear ODE system

We begin with the simplest class of dynamical systems to test SINDy-KANs. Even though these equations can be discovered by simpler methods, such as dynamic model discovery, it is useful to confirm that simple systems are also properly identified with the more general SINDy-KAN infrastructure.

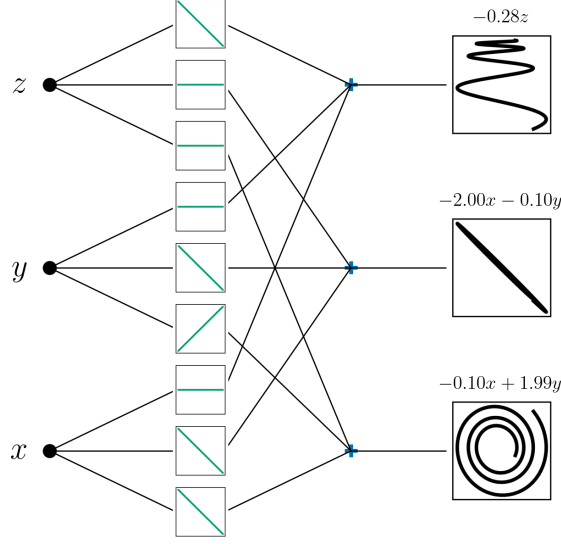


Figure 4: Trained SINDy-KAN for Sec. 4.2.1.

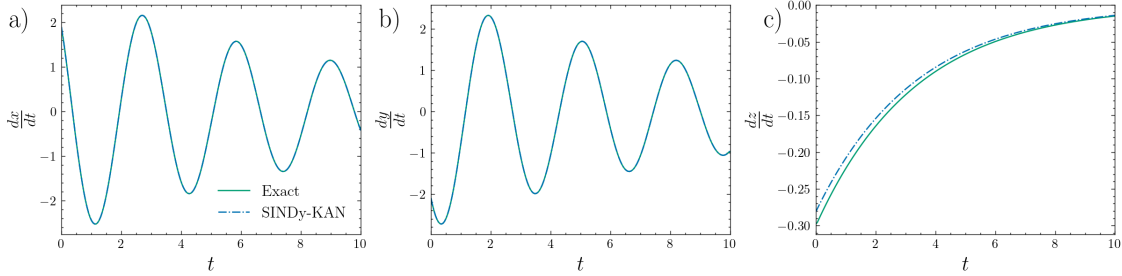


Figure 5: Trained SINDy-KAN for Sec. 4.2.1. The SINDy-KAN results agree well with the data.

We consider the 3D system of equations

$$\frac{d}{dt} \begin{bmatrix} x \\ y \\ z \end{bmatrix} = \begin{bmatrix} -0.1 & 2 & 0 \\ -2 & -0.1 & 0 \\ 0 & 0 & -0.3 \end{bmatrix} \begin{bmatrix} x \\ y \\ z \end{bmatrix}. \quad (19)$$

We take the library of candidate functions $\Theta_{\ell,j,i}(\mathbf{x})$ as polynomials up to degree three,

$$\Theta_{\ell,i} = \begin{bmatrix} | & | & | & | \\ \mathbf{1} & \mathbf{X}_i^{(\ell)} & \mathbf{X}_i^{(\ell)^2} & \mathbf{X}_i^{(\ell)^3} \\ | & | & | & | \end{bmatrix}. \quad (20)$$

The training data is generated with `pysindy` [60, 61, 62]. Data is generated at 200 evenly spaced points in the interval $t \in [0, 10]$.

The SINDy-KAN learns the equation

$$\frac{d}{dt} \begin{bmatrix} x \\ y \\ z \end{bmatrix} = \begin{bmatrix} -0.0993 & 1.9946 & 0 \\ -1.9972 & -0.0995 & 0 \\ 0 & 0 & -0.2811 \end{bmatrix} \begin{bmatrix} x \\ y \\ z \end{bmatrix}. \quad (21)$$

The trained SINDy-KAN is given in Fig. 4 and the results are shown in Fig. 5. We extend this case to consider training with noise in Appendix B.

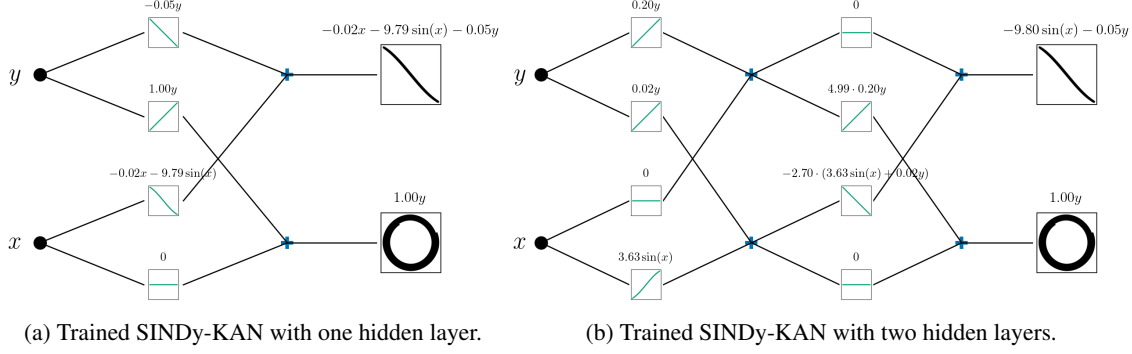


Figure 6: Trained SINDy-KANs for the pendulum in Sec. 4.2.2 with one (a) and two (b) hidden layers.

4.2.2 Damped pendulum

We consider a damped pendulum with equation given by:

$$\frac{dx}{dt} = y \quad (22)$$

$$\frac{dy}{dt} = -0.05y - 9.81 \sin(x) \quad (23)$$

and the library of candidate functions

$$\Theta_{\ell,i} = \left[\begin{array}{c} | \\ | \\ \mathbf{1} \\ | \\ \mathbf{X}_i^{(\ell)} \\ | \\ \mathbf{X}_i^{(\ell)^2} \\ | \\ \sin(\mathbf{X}_i^{(\ell)}) \\ | \\ \cos(\mathbf{X}_i^{(\ell)}) \\ | \end{array} \right]. \quad (24)$$

We can use this test to examine the performance of SINDy-KANs when the architecture is varied by considering SINDy-KANs with one and two hidden activation function layers. The training data is found by numerically solving Eqs. 22 and 23 at 1000 points in the time interval $t \in [0, 10]$.

The SINDy-KAN with one hidden layer learns

$$\begin{aligned} \frac{dx}{dt} &= 0.9998y \\ \frac{dy}{dt} &= -9.7877 \sin(x) - 0.0499y - 0.0185x. \end{aligned}$$

The SINDy-KAN with two hidden layers learns

$$\begin{aligned} \frac{dx}{dt} &= 0.9997y \\ \frac{dy}{dt} &= -9.7975 \sin(x) - 0.0499y. \end{aligned}$$

Plots of the trained SINDy-KAN are shown in fig. 6a, fig. 6b and fig. 7. The deeper SINDy-KAN is slightly more accurate due to the additional flexibility of the extra hidden layer. However, deeper KANs can also be harder to train in general [63], so there is a trade off between the additional flexibility, training time, and complexity of training.

4.2.3 ABC flow

When dynamics of the problem are known they can be incorporated into the SINDy-KAN candidate functions to improve training. For an example, we consider the ABC flow example inspired by [42], given by

$$\frac{dx}{dt} = A \sin(w_1 z) + C \cos(w_2 y) \quad (25)$$

$$\frac{dy}{dt} = B \sin(w_3 x) + A \cos(w_4 z) \quad (26)$$

$$\frac{dz}{dt} = C \sin(w_5 y) + B \cos(w_6 x) \quad (27)$$

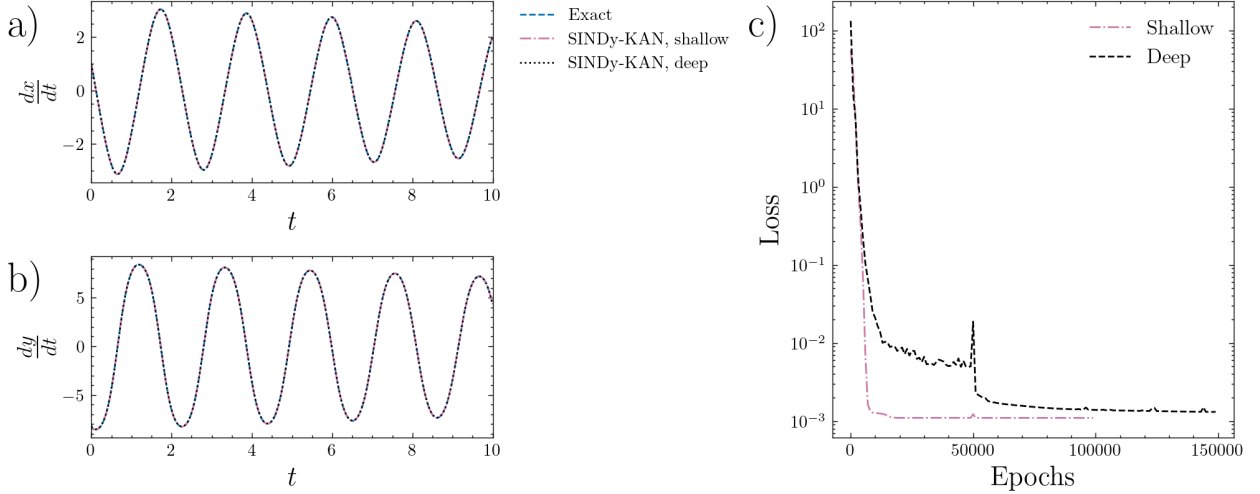


Figure 7: SINDy-KAN results for Sec. 4.2.2. (a-b) Results for the SINDy-KANs, compared with the numerical derivatives. (c) Loss for the SINDy-KAN.

for $A = 2$, $B = 3$, $C = 1$, and $w_1 = \pi/4.0$, $w_2 = \pi/3.0$, $w_3 = \pi/2.0$, $w_4 = \pi/5.0$, $w_5 = \pi/4.5$, $w_6 = \pi/2.8$. We use this equation to highlight the selection of different candidate functions for each hidden layer in the KAN. If we know the equations are of the form $\sum_{i=1}^3 a_i \sin(w_i x_i) + b_i \cos(v_i x_i)$ for $i \in \{1, 2, 3\}$ and unknown coefficients a_i , b_i , w_i and v_i , we can consider a two layer KAN, with the candidate functions for the first layer $\{x\}$ and the candidate functions for the second layer $\{\cos(x), \sin(x)\}$. By keeping the first layer as a linear basis to learn the right coordinates/scaling, then feeding them into the nonlinear terms, we restrict the training space to allow for better training while capturing the dynamics of the problem. We emphasize that the frequencies w_i are learned by the SINDy-KAN instead of prescribed by the user. The training data are found by numerically solving the system of equations at 20000 points in the time interval $t \in [0, 20]$.

Eqns. 25-27 give approximately:

$$\begin{aligned} \frac{dx}{dt} &= 2 \sin(0.7854z) + 1 \cos(1.0472y) \\ \frac{dy}{dt} &= 3 \sin(1.5708x) + 2 \cos(0.6283z) \\ \frac{dz}{dt} &= 1 \sin(0.6981y) + 3 \cos(1.1210x). \end{aligned}$$

With the SINDy-KAN, we learn:

$$\begin{aligned} \frac{dx}{dt} &= 2.0072 \sin(0.7849z) + 1.0000 \cos(1.0470y) \\ \frac{dy}{dt} &= 2.9990 \sin(1.5708x) + 1.9926 \cos(0.6278z) \\ \frac{dz}{dt} &= 0.9996 \sin(0.6976y) + 2.9983 \cos(1.2221x). \end{aligned}$$

The trained SINDy-KAN is shown in Fig. 8 and the results from the SINDy-KAN are shown in Fig. 9. As in [42], SINDy-KANs are able to directly learn the frequencies accurately. This presents a strong advantage over standard SINDy, where the frequencies would need to be predetermined to be included in the library of candidate functions.

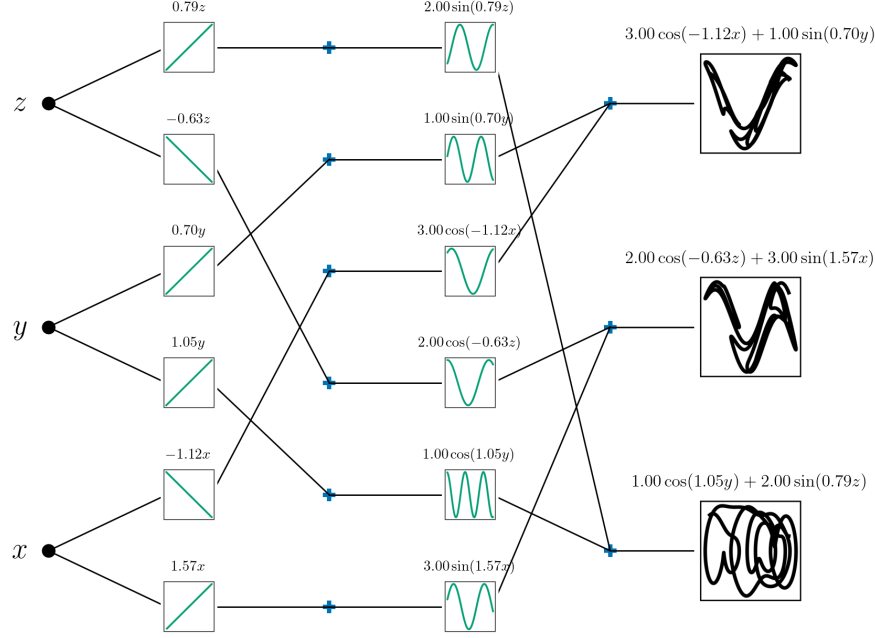


Figure 8: The SINDy-KAN for ABC flow problem in Sec. 4.2.3. For clarity, only the non-zero activation functions are shown.

4.2.4 Lorenz

We next consider the nonlinear Lorenz system

$$\frac{dx}{dt} = \sigma(y - x) \quad (28)$$

$$\frac{dy}{dt} = x(\rho - z) - y \quad (29)$$

$$\frac{dz}{dt} = xy - \beta z \quad (30)$$

for $\rho = 28.0$, $\sigma = 10.0$, and $\beta = 8.0/3.0 \approx 2.6667$. This example highlights the use of multiplication SINDy-KANs. In particular, we use a KAN with one hidden layer with five nodes, and take two of the nodes as multiplication nodes ($n_1^m = 2$). We take the library of candidate functions for the activation functions as polynomials up to degree one,

$$\Theta_{\ell,i} = \begin{bmatrix} | \\ \mathbf{1} & \mathbf{X}_i^{(\ell)} \\ | \end{bmatrix}. \quad (31)$$

With the multiplication nodes, the multiplication KAN can represent second degree polynomials after the first layer, even though each activation function is univariate. In contrast, a standard KAN would take two hidden layers to represent second degree polynomials.

We train the SINDy-KAN using data generated with the initial condition $(-8, 8, 27)$. The training data is found by numerically solving the system of equations at 5000 points in the time interval $t \in [0, 10]$.

The SINDy-KAN learns:

$$\frac{dx}{dt} = -10.00001x + 9.99999y \quad (32)$$

$$\frac{dy}{dt} = x(28.00002 - 1.00000z) - 1.00000y \quad (33)$$

$$\frac{dz}{dt} = 1.00000xy - 2.66666z. \quad (34)$$

The results are plotted in Fig. 10 and the trained KAN is shown in Fig. 11.

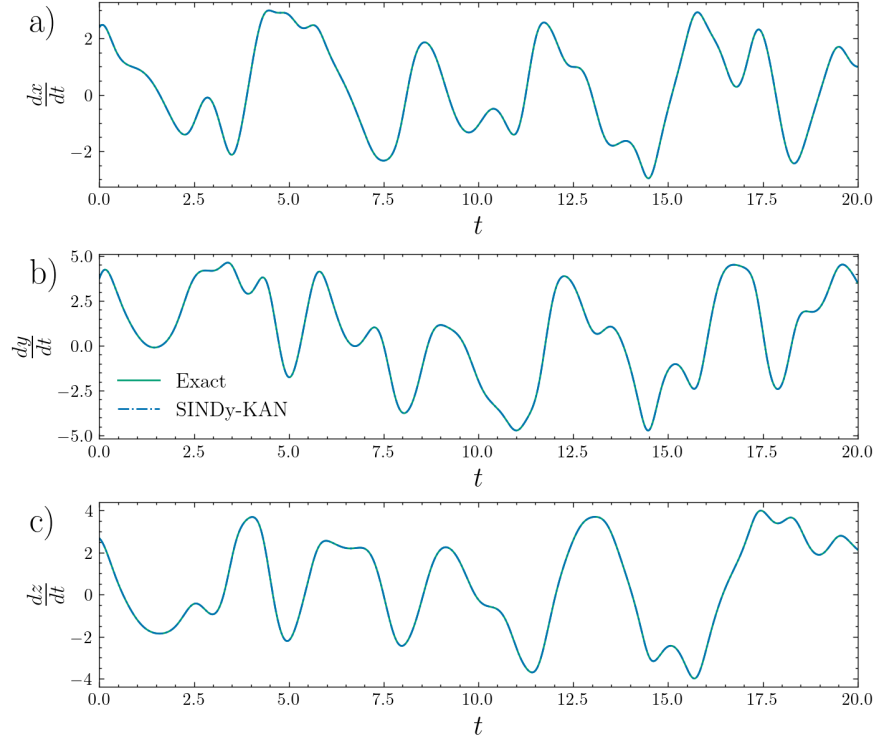


Figure 9: The SINDy-KAN learns the dynamics of the ABC flow problem in Sec. 4.2.3 well.

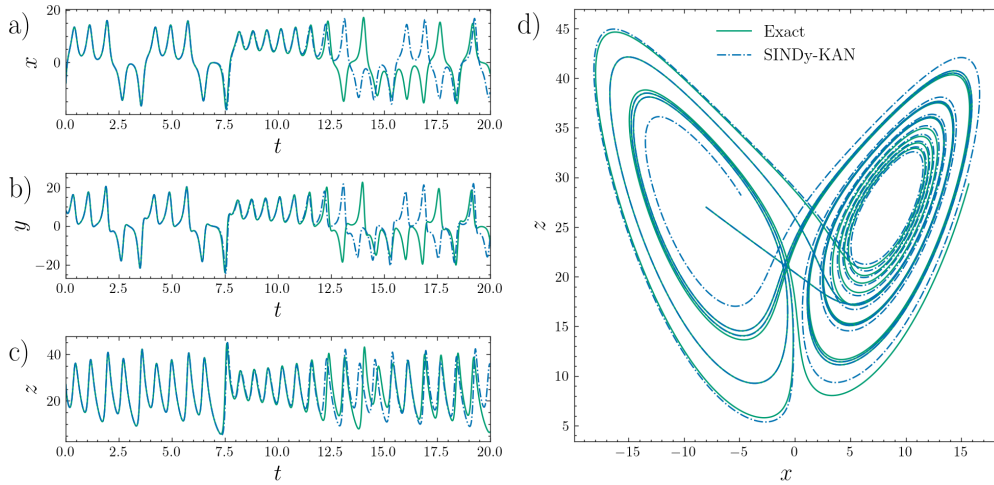


Figure 10: The Lorenz system in Eqs. 28–30 and the system learned by the SINDy-KAN in Eqs. 32–34 for Sec. 4.2.4. Both the true system and the learned system are evaluated numerically. We note that only data from $t \in [0, 10]$ is used for training.

4.2.5 Kuramoto oscillator

The Kuramoto oscillator is defined by

$$\frac{d\theta_i}{dt} = \omega_i + \frac{1}{N} \sum_{j=1}^N K_{ij} \sin(\theta_j - \theta_i), \quad i = 1, \dots, N. \quad (35)$$

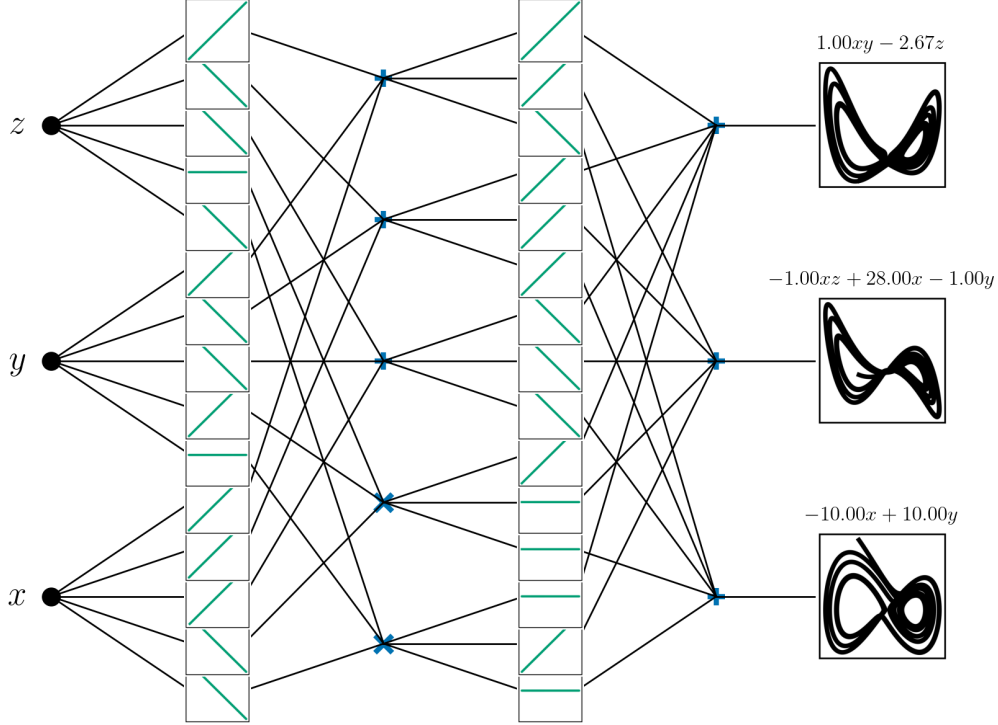


Figure 11: The trained SINDy-KAN for the Lorenz system in Sec. 4.2.4. Multiplication nodes are denoted by “ \times ” and addition nodes are denoted by “ $+$ ”.

We consider $N = 3$ and $\omega_1 = 16$, $\omega_2 = 5$, and $\omega_3 = 11$ with $K_{ij} = 1$ for all i, j . We consider a two layer KAN, with the candidate functions for the first layer $\{x\}$ and the candidate functions for the second layer $\{1, \sin(x)\}$. The training data is generated with [64] at 5000 points for $t \in [0, 5]$.

The SINDy-KAN learns

$$\frac{d\theta_1}{dt} = -1.0002 \sin(0.9988\theta_1 - 0.9985\theta_3) - 1.0001 \sin(0.9994\theta_1 - 0.9981\theta_2) + 15.9995 \quad (36)$$

$$\frac{d\theta_2}{dt} = 1.0000 \sin(0.9994\theta_1 - 0.9981\theta_2) - 1.0002 \sin(0.9988\theta_2 - 0.9990\theta_3) + 5.0002 \quad (37)$$

$$\frac{d\theta_3}{dt} = 1.0001 \sin(0.9988\theta_1 - 0.9985\theta_3) + 1.0002 \sin(0.9988\theta_2 - 0.9990\theta_3) + 11.0003. \quad (38)$$

Examining the KAN structure in Fig. 12, the KAN uses only three of the six nodes in the hidden layer (the other nodes are zero.) This minimizes the ℓ_1 penalty $\lambda_1 \|\Lambda\|_1$ in the loss function by reusing the $\theta_i - \theta_j$ terms in the final equations by recognizing the symmetry that $\sin(x) = -\sin(-x)$.

5 Conclusions

We have shown SINDy-KANs train well and accurately discover equations for a variety of datasets, including chaotic dynamical systems. SINDy-KANs can learn compositions of functions that are difficult to learn with SINDy, where the exact needed composition may not be included in the function library. At the same time, SINDy-KANs more robustly learn parsimonious representations than standard KANs. This combination of function compositions and sparse function representations builds on the strengths of both KANs and SINDy in a harmonious way to offer increased symbolic regression. More broadly, SINDy-KANs contribute to the growing effort to develop interpretable and trustworthy machine learning methods for scientific discovery. By enforcing parsimony at the level of each activation function while retaining the expressiveness of deep networks, SINDy-KANs offer a principled framework for learning human-readable equations from data.

Despite these strengths, several limitations remain. As the number of input variables grows, the interpretability of the discovered equations may diminish, a challenge shared with standard KAN-based symbolic regression. Additionally,

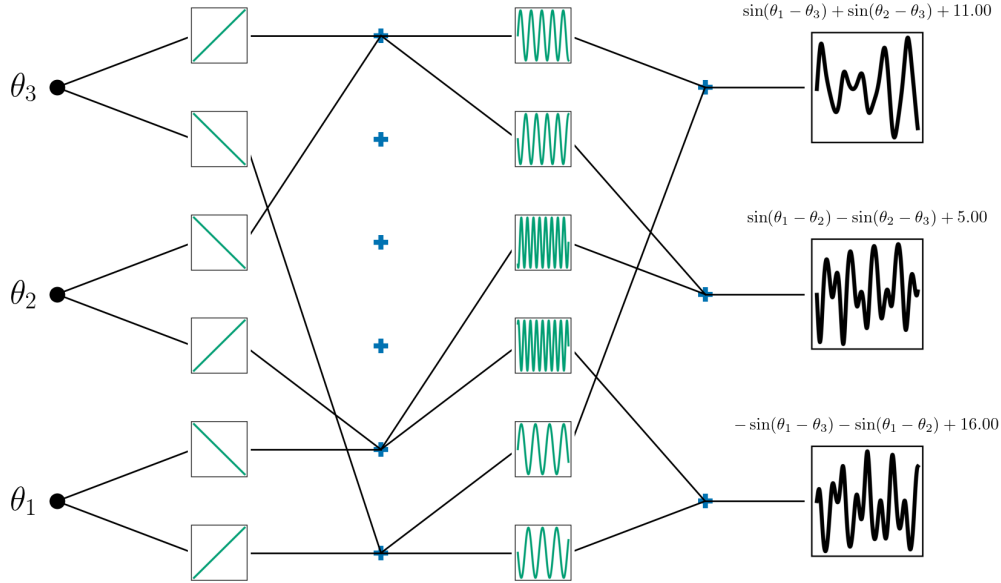


Figure 12: The trained SINDy-KAN for the Kuramoto system in Sec. 4.2.5. Multiplication nodes are denoted by “ \times ” and addition nodes are denoted by “ $+$ ”. For clarity, only non-zero nodes are shown.

discovering dynamical systems from data requires numerical differentiation, which can be sensitive to noise. While methods such as finite differences have been successfully applied in SINDy, further work is needed to evaluate the robustness of SINDy-KANs under noisy conditions.

The examples in this work are all trained on a single Apple M3 Max Macbook Pro, generally in less than a few minutes per problem. Due to not needing to complete the sparse regression at each activation function for each iteration, the direct SINDy-KANs presented in Appendix A train significantly faster. However, SINDy-KANs do not represent a large computational burden. Due to the comparable accuracy between the two approaches, we suggest the faster training times are an argument to use direct SINDy-KANs when possible. However, direct SINDy-KANs assume that each activation function can be represented well by linear combinations of the library functions. In future work, we will consider cases where some activation functions can be kept as their B-spline representations, while others are fixed by their symbolic forms based on the error while training. This will allow for accuracy when the set of library functions is not sufficient to capture the system dynamics. For this approach, SINDy-KANs are necessary.

One consideration when training SINDy-KANs is the network architecture. The depth of the network is the number of function compositions that can occur, and it is difficult to know the necessary number of layers in advance. While SINDy-KANs can learn the identity function for additional unneeded layers, multi-exit KANs could be combined with SINDy-KANs to simultaneously learn the best network architecture and symbolic representation [63]. Beyond those considered in this work, SINDy-KANs could be combined with many other KAN training schemes to increase accuracy [18], including domain decomposition if different equations are expected in different parts of the domain [65], adaptive weighting schemes [66], automatic grid updates [67], or improved optimizers [6]. Improved training of the underlying KAN improves the accuracy of the learned equations.

6 Acknowledgments

This project was completed with support from the U.S. Department of Energy, Advanced Scientific Computing Research program, under the Scalable, Efficient and Accelerated Causal Reasoning Operators, Graphs and Spikes for Earth and Embedded Systems (SEA-CROGS) project (Project No. 80278). The computational work was performed using PNNL Institutional Computing at Pacific Northwest National Laboratory. Pacific Northwest National Laboratory (PNNL) is a multi-program national laboratory operated for the U.S. Department of Energy (DOE) by Battelle Memorial Institute under Contract No. DE-AC05-76RL01830. SLB and NZ acknowledge funding support from the National Science Foundation AI Institute in Dynamic Systems (grant number 2112085).

7 Data and code availability

The examples in this work were developed using the `jaxKAN` package [68, 69]. Results were compared with symbolic regression using `pykan` [1]. Postprocessing of the learned equations was performed with `sympy` [70].

All code and data will be released upon publication.

References

- [1] Ziming Liu, Yixuan Wang, Sachin Vaidya, Fabian Ruehle, James Halverson, Marin Soljačić, Thomas Y Hou, and Max Tegmark. KAN: Kolmogorov-Arnold networks. *arXiv preprint arXiv:2404.19756*, 2024.
- [2] Ziming Liu, Pingchuan Ma, Yixuan Wang, Wojciech Matusik, and Max Tegmark. KAN 2.0: Kolmogorov-Arnold networks meet science. *arXiv preprint arXiv:2408.10205*, 2024.
- [3] Khemraj Shukla, Juan Diego Toscano, Zhicheng Wang, Zongren Zou, and George Em Karniadakis. A comprehensive and FAIR comparison between MLP and KAN representations for differential equations and operator networks. *Computer Methods in Applied Mechanics and Engineering*, 431:117290, 2024.
- [4] Yizheng Wang, Jia Sun, Jinshuai Bai, Cosmin Anitescu, Mohammad Sadegh Eshaghi, Xiaoying Zhuang, Timon Rabczuk, and Yinghua Liu. Kolmogorov-Arnold-Informed neural network: A physics-informed deep learning framework for solving forward and inverse problems based on Kolmogorov-Arnold networks. *Computer Methods in Applied Mechanics and Engineering*, 433:117518, 2025.
- [5] Salah A Faroughi, Farinaz Mostajeran, Amin Hamed Mashhadzadeh, and Shirko Faroughi. Scientific machine learning with kolmogorov-arnold networks. *arXiv preprint arXiv:2507.22959*, 2025.
- [6] Elham Kiyani, Khemraj Shukla, Jorge F Urbán, Jérôme Darbon, and George Em Karniadakis. Which optimizer works best for physics-informed neural networks and kolmogorov-arnold networks? *arXiv preprint arXiv:2501.16371*, 2025.
- [7] Mehrdad Kiamari, Mohammad Kiamari, and Bhaskar Krishnamachari. GKAN: Graph Kolmogorov-Arnold Networks. *arXiv preprint arXiv:2406.06470*, 2024.
- [8] Gianluca De Carlo, Andrea Mastropietro, and Aris Anagnostopoulos. Kolmogorov-Arnold Graph Neural Networks. *arXiv preprint arXiv:2406.18354*, 2024.
- [9] Roman Bresson, Giannis Nikolentzos, George Panagopoulos, Michail Chatzianastasis, Jun Pang, and Michalis Vazirgiannis. KAGNNs: Kolmogorov-Arnold networks meet graph learning. *Transactions on Machine Learning Research*, 2025.
- [10] Diab W Abueidda, Panos Pantidis, and Mostafa E Mobasher. DeepOKAN: Deep operator network based on Kolmogorov-Arnold networks for mechanics problems. *Computer Methods in Applied Mechanics and Engineering*, 436:117699, 2025.
- [11] Maziar Raissi, Paris Perdikaris, and George E Karniadakis. Physics-informed neural networks: A deep learning framework for solving forward and inverse problems involving nonlinear partial differential equations. *Journal of Computational Physics*, 378:686–707, 2019.
- [12] Minjong Cheon. Kolmogorov-Arnold Network for satellite image classification in remote sensing. *arXiv preprint arXiv:2406.00600*, 2024.
- [13] Cristian J Vaca-Rubio, Luis Blanco, Roberto Pereira, and Mărius Caus. Kolmogorov-Arnold networks (KANs) for time series analysis. *arXiv preprint arXiv:2405.08790*, 2024.
- [14] Juan Diego Toscano, Theo Käufer, Martin Maxey, Christian Cierpka, and George Em Karniadakis. Inferring turbulent velocity and temperature fields and their statistics from Lagrangian velocity measurements using physics-informed Kolmogorov-Arnold networks. *arXiv preprint arXiv:2407.15727*, 2024.
- [15] Ali Kashefi. Kolmogorov-Arnold PointNet: Deep learning for prediction of fluid fields on irregular geometries. *Computer Methods in Applied Mechanics and Engineering*, 439:117888, 2025.
- [16] Xiong Xiong, Kang Lu, Zhuo Zhang, Zheng Zeng, Sheng Zhou, Zichen Deng, and Rongchun Hu. J-pikan: A physics-informed kan network based on jacobi orthogonal polynomials for solving fluid dynamics. *Communications in Nonlinear Science and Numerical Simulation*, page 109414, 2025.
- [17] Shriyank Somvanshi, Syed Aaqib Javed, Md Monzurul Islam, Diwas Pandit, and Subasish Das. A survey on kolmogorov-arnold network. *ACM Computing Surveys*, 58(2):1–35, 2025.
- [18] Amir Noorizadegan, Sifan Wang, and Leevan Ling. A practitioner’s guide to kolmogorov-arnold networks. *arXiv preprint arXiv:2510.25781*, 2025.

- [19] Juan Diego Toscano, Vivek Oommen, Alan John Varghese, Zongren Zou, Nazanin Ahmadi Daryakenari, Chenxi Wu, and George Em Karniadakis. From pinns to pikans: Recent advances in physics-informed machine learning. *Machine Learning for Computational Science and Engineering*, 1(1):15, 2025.
- [20] Irina Barašin, Blaž Bertalanič, Mihael Mohorčič, and Carolina Fortuna. Exploring kolmogorov–arnold networks for interpretable time series classification. *International Journal of Intelligent Systems*, 2025(1):9553189, 2025.
- [21] Nataly R Panczyk, Omer F Erdem, and Majdi I Radaideh. Opening the black-box: Symbolic regression with kolmogorov-arnold networks for energy applications. *arXiv preprint arXiv:2504.03913*, 2025.
- [22] Hanyu Gao, Aoxue Wang, Zhenlin Ouyang, Zhaohui Li, and Xiaoliang Chen. Toward intrinsically interpretable ai in optical networks using kan-based symbolic regression. In *2024 IEEE Future Networks World Forum (FNWF)*, pages 26–31. IEEE, 2024.
- [23] Cunyi Liao, Xinyue Ge, Mingjian He, Yi Zheng, and Shouyin Liu. Kan based interpretable radio map prediction framework with symbolic data fusion. *IEEE Transactions on Cognitive Communications and Networking*, 2025.
- [24] Yanhong Peng, Yuxin Wang, Fangchao Hu, Miao He, Zebing Mao, Xia Huang, and Jun Ding. Predictive modeling of flexible ehd pumps using kolmogorov–arnold networks. *Biomimetic Intelligence and Robotics*, 4(4):100184, 2024.
- [25] Kunhua Zhong, Yuwen Chen, Wenqiang Yang, Jingyu Chen, Peng Tang, Peng Wang, and Jiang Liu. Interpretable disease prediction based on kolmogorov-arnold networks. In *2024 IEEE International Conference on Medical Artificial Intelligence (MedAI)*, pages 645–650. IEEE, 2024.
- [26] Isabela Suaza-Sierra, Hernan A Moreno, Luis A De la Fuente, and Thomas M Neeson. Interpretable machine learning for reservoir water temperatures in the us red river basin of the south. *arXiv preprint arXiv:2511.01837*, 2025.
- [27] Thomas R Harvey, Fabian Ruehle, Kit Fraser-Taliente, and James Halverson. Symbolic regression with multimodal large language models and kolmogorov arnold networks. *arXiv preprint arXiv:2505.07956*, 2025.
- [28] Marco Andrea Bühler and Gonzalo Guillén-Gosálbez. Kan-sr: A kolmogorov-arnold network guided symbolic regression framework. *arXiv preprint arXiv:2509.10089*, 2025.
- [29] James Bagrow and Josh Bongard. Softly symbolifying kolmogorov-arnold networks. *arXiv preprint arXiv:2512.07875*, 2025.
- [30] Steven L Brunton, Joshua L Proctor, and J Nathan Kutz. Discovering governing equations from data by sparse identification of nonlinear dynamical systems. *Proceedings of the national academy of sciences*, 113(15):3932–3937, 2016.
- [31] Sarah Beetham and Jesse Capecehatro. Formulating turbulence closures using sparse regression with embedded form invariance. *Physical Review Fluids*, 5(8):084611, 2020.
- [32] Sarah Beetham, Rodney O Fox, and Jesse Capecehatro. Sparse identification of multiphase turbulence closures for coupled fluid–particle flows. *Journal of Fluid Mechanics*, 914:A11, 2021.
- [33] Niall M Mangan, Steven L Brunton, Joshua L Proctor, and J Nathan Kutz. Inferring biological networks by sparse identification of nonlinear dynamics. *IEEE Transactions on Molecular, Biological, and Multi-Scale Communications*, 2(1):52–63, 2017.
- [34] Eurika Kaiser, J Nathan Kutz, and Steven L Brunton. Sparse identification of nonlinear dynamics for model predictive control in the low-data limit. *Proceedings of the Royal Society A*, 474(2219):20180335, 2018.
- [35] Nicholas Zolman, Christian Lagemann, Urban Fasel, J Nathan Kutz, and Steven L Brunton. Sindy-rl for interpretable and efficient model-based reinforcement learning. *Nature Communications*, 16(1):10714, 2025.
- [36] Urban Fasel, J Nathan Kutz, Bingni W Brunton, and Steven L Brunton. Ensemble-sindy: Robust sparse model discovery in the low-data, high-noise limit, with active learning and control. *Proceedings of the Royal Society A*, 478(2260):20210904, 2022.
- [37] Hayden Schaeffer and Scott G McCalla. Sparse model selection via integral terms. *Physical Review E*, 96(2):023302, 2017.
- [38] Patrick AK Reinbold, Daniel R Gurevich, and Roman O Grigoriev. Using noisy or incomplete data to discover models of spatiotemporal dynamics. *Physical Review E*, 101(1):010203, 2020.
- [39] Daniel A Messenger and David M Bortz. Weak SINDy for partial differential equations. *Journal of Computational Physics*, 443:110525, 2021.
- [40] Daniel A Messenger and David M Bortz. Weak SINDy: Galerkin-based data-driven model selection. *Multiscale Modeling & Simulation*, 19(3):1474–1497, 2021.

- [41] Pawan Goyal and Peter Benner. Discovery of nonlinear dynamical systems using a runge–kutta inspired dictionary-based sparse regression approach. *Proceedings of the Royal Society A*, 478(2262):20210883, 2022.
- [42] Siva Viknesh, Younes Tatari, Chase Christenson, and Amirhossein Arzani. Adam-sindy: An efficient optimization framework for parameterized nonlinear dynamical system identification. *Physical Review Research*, 8(1):013040, 2026.
- [43] Diederik P Kingma. Adam: A method for stochastic optimization. *arXiv preprint arXiv:1412.6980*, 2014.
- [44] Benjamin C Koenig, Suyong Kim, and Sili Deng. Leankan: A parameter-lean kolmogorov-arnold network layer with improved memory efficiency and convergence behavior. *arXiv preprint arXiv:2502.17844*, 2025.
- [45] J.-C. Loiseau and S. L. Brunton. Constrained sparse Galerkin regression. *Journal of Fluid Mechanics*, 838:42–67, 2018.
- [46] Alan A Kaptanoglu, Kyle D Morgan, Chris J Hansen, and Steven L Brunton. Physics-constrained, low-dimensional models for mhd: First-principles and data-driven approaches. *Physical Review E*, 104(015206), 2021.
- [47] Jared L Callaham, J-C Loiseau, Georgios Rigas, and Steven L Brunton. Nonlinear stochastic modelling with Langevin regression. *Proceedings of the Royal Society A*, 477(2250):20210092, 2021.
- [48] Yifei Guan, Steven L Brunton, and Igor Novosselov. Sparse nonlinear models of chaotic electroconvection. *Royal Society Open Science*, 8(8):202367, 2021.
- [49] Jean-Christophe Loiseau. Data-driven modeling of the chaotic thermal convection in an annular thermosyphon. *Theoretical and Computational Fluid Dynamics*, 34, 2020.
- [50] Nan Deng, Bernd R Noack, Marek Morzyński, and Luc R Pastur. Galerkin force model for transient and post-transient dynamics of the fluidic pinball. *Journal of Fluid Mechanics*, 918, 2021.
- [51] Jared L Callaham, Steven L Brunton, and Jean-Christophe Loiseau. On the role of nonlinear correlations in reduced-order modeling. *Journal of Fluid Mechanics*, 938(A1), 2022.
- [52] Jared L Callaham, Georgios Rigas, Jean-Christophe Loiseau, and Steven L Brunton. An empirical mean-field model of symmetry-breaking in a turbulent wake. *Science Advances*, 8(eabm4786), 2022.
- [53] Laure Zanna and Thomas Bolton. Data-driven equation discovery of ocean mesoscale closures. *Geophysical Research Letters*, 47(17):e2020GL088376, 2020.
- [54] Martin Schmelzer, Richard P Dwight, and Paola Cinnella. Discovery of algebraic Reynolds-stress models using sparse symbolic regression. *Flow, Turbulence and Combustion*, 104(2):579–603, 2020.
- [55] Spyros Rigas and Michalis Papachristou. jaxkan: A unified jax framework for kolmogorov-arnold networks. *Journal of Open Source Software*, 10(108):7830, 2025.
- [56] Spyros Rigas, Dhruv Verma, Georgios Alexandridis, and Yixuan Wang. Initialization schemes for kolmogorov-arnold networks: An empirical study. *arXiv preprint arXiv:2509.03417*, 2025.
- [57] Spyros Rigas, Michalis Papachristou, Theofilos Papadopoulos, Fotios Anagnostopoulos, and Georgios Alexandridis. Adaptive training of grid-dependent physics-informed Kolmogorov-Arnold networks. *IEEE Access*, 2024.
- [58] Spyros Rigas, Fotios Anagnostopoulos, Michalis Papachristou, and Georgios Alexandridis. Towards deep physics-informed kolmogorov-arnold networks. *arXiv preprint arXiv:2510.23501*, 2025.
- [59] Sidharth SS, Keerthana AR, Gokul R, and Anas KP. Chebyshev polynomial-based Kolmogorov-Arnold networks: An efficient architecture for nonlinear function approximation. *arXiv preprint arXiv:2405.07200*, 2024.
- [60] Brian de Silva, Kathleen Champion, Markus Quade, Jean-Christophe Loiseau, J. Kutz, and Steven Brunton. Pysindy: A python package for the sparse identification of nonlinear dynamical systems from data. *Journal of Open Source Software*, 5(49):2104, 2020.
- [61] Alan A. Kaptanoglu, Brian M. de Silva, Urban Fasel, Kadierdan Kaheman, Andy J. Goldschmidt, Jared Callaham, Charles B. Delahunt, Zachary G. Nicolaou, Kathleen Champion, Jean-Christophe Loiseau, J. Nathan Kutz, and Steven L. Brunton. Pysindy: A comprehensive python package for robust sparse system identification. *Journal of Open Source Software*, 7(69):3994, 2022.
- [62] Alan Kaptanoglu, Jacob Stevens-Haas, Kathleen Champion, Brian de Silva, and Markus Quade. pysindy.
- [63] James Bagrow and Josh Bongard. Multi-exit kolmogorov–arnold networks: enhancing accuracy and parsimony. *Machine Learning: Science and Technology*, 6(3):035037, August 2025.
- [64] D. Laszuk. Python implementation of kuramoto systems. <http://www.laszukdawid.com/codes>, 2017.

-
- [65] Amanda A. Howard, Bruno Jacob, Sarah Helfert, Alexander Heinlein, and Panos Stinis. Finite basis kolmogorov-arnold networks: domain decomposition for data-driven and physics-informed problems. *arXiv preprint arXiv:2406.19662*, 2025.
- [66] Sokratis J Anagnostopoulos, Juan Diego Toscano, Nikolaos Stergiopoulos, and George Em Karniadakis. Residual-based attention in physics-informed neural networks. *Computer Methods in Applied Mechanics and Engineering*, 421:116805, 2024.
- [67] Jamison Moody and James Usevitch. Automatic grid updates for kolmogorov-arnold networks using layer histograms. *arXiv preprint arXiv:2511.08570*, 2025.
- [68] Spyros Rigas and Michalis Papachristou. jaxKAN: A JAX-based implementation of Kolmogorov-Arnold Networks, May 2024.
- [69] Spyros Rigas and Michalis Papachristou. jaxKAN: A unified JAX framework for Kolmogorov-Arnold networks. *Journal of Open Source Software*, 10(108):7830, 2025.
- [70] Aaron Meurer, Christopher P. Smith, Mateusz Paprocki, Ondřej Čertík, Sergey B. Kirpichev, Matthew Rocklin, Amit Kumar, Sergiu Ivanov, Jason K. Moore, Sartaj Singh, Thilina Rathnayake, Sean Vig, Brian E. Granger, Richard P. Muller, Francesco Bonazzi, Harsh Gupta, Shivam Vats, Fredrik Johansson, Fabian Pedregosa, Matthew J. Curry, Andy R. Terrel, Štěpán Roučka, Ashutosh Saboo, Isuru Fernando, Sumith Kulal, Robert Cimrman, and Anthony Scopatz. Sympy: symbolic computing in python. *PeerJ Computer Science*, 3:e103, January 2017.

	$\mathcal{K}_\Lambda^{direct}$	\mathcal{K}_Λ (From Sec. 4.1)
Exact eq. $f(x, y) = \cos(x^2 + y)$	$0.99986 \cos(0.99996x^2 + 0.99995y)$	$0.99990 \cos(1.00001x^2 + 0.99994y)$
Training time (s)	145	215

Table 1: Comparison of SINDy-KANs and direct SINDy-KANs.

	$\mathcal{K}_\Lambda^{direct}$	\mathcal{K}_Λ (From Sec. 4.2.1)
$\mathbf{B} = \begin{bmatrix} -0.1 & 2 & 0 \\ -2 & -0.1 & 0 \\ 0 & 0 & -0.3 \end{bmatrix}$	$\begin{bmatrix} -0.0989 & 1.9941 & 0 \\ -1.9967 & -0.0989 & 0 \\ 0 & 0 & -0.2964 \end{bmatrix}$	$\begin{bmatrix} -0.0993 & 1.9946 & 0 \\ -1.9972 & -0.0995 & 0 \\ 0 & 0 & -0.2811 \end{bmatrix}$

Table 2: Comparison of SINDy-KANs and direct SINDy-KANs for the ODE problem in Sec. 4.2.1.

A Direct SINDy-KANs

In direct SINDy-KANs, the coefficients Ξ_S are taken as trainable parameters and learned directly (the underlying KAN is not trained.) Direct SINDy-KANs can be thought of as a deep version of ADAM-SINDy [42], where instead of learning one set of coefficients, the coefficients for each activation function in a KAN are learned through the ADAM optimizer. Alternatively, direct SINDy-KANs are directly equivalent to Softly Symbolified Kolmogorov-Arnold Networks (S2KANs), with a different method of enforcing sparsity.

In direct SINDy-KANs, eq. (16) is modified to

$$\mathcal{L}_{direct} = \lambda_S \mathcal{L}_S + \lambda_\Lambda \mathcal{L}_\Lambda + \lambda_1 \|\mathbf{A}\|_1 + \lambda_2 \|\mathbf{A} - \Xi_S\|_2^2 \quad (39)$$

where the term \mathcal{L}_{KAN} is removed, since there is no longer an underlying KAN to optimize.

Direct SINDy-KANs can be significantly faster than indirect SINDy-KANs because the method does not require solving a least squares problem at each activation function during each iteration. From Table 1, this corresponds to about a 33% reduction in the computational cost for training for the example problem from Sec. 4.1. However, in our tests, direct SINDy-KANs can be more challenging to train than SINDy-KANs as presented above. For this reason, we present some results with direct SINDy-KANs here, and leave further exploration of the stability and convergence of training direct SINDy-KANs for future work.

We can also consider the ODE case from Sec. 4.2.1, given by

$$\frac{d}{dt} \begin{bmatrix} x \\ y \\ z \end{bmatrix} = \mathbf{B} \begin{bmatrix} x \\ y \\ z \end{bmatrix} \quad (40)$$

where

$$\mathbf{B} = \begin{bmatrix} -0.1 & 2 & 0 \\ -2 & -0.1 & 0 \\ 0 & 0 & -0.3 \end{bmatrix}. \quad (41)$$

From Table 2, the SINDy-KANs and direct SINDy-KANs have comparable performance.

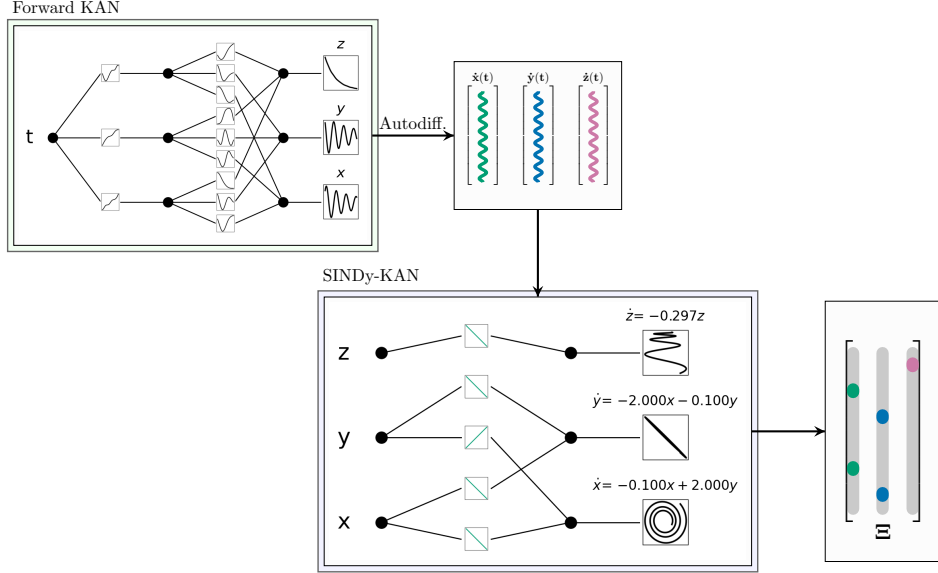


Figure 13: An illustration of SINDy-KANs for dynamical systems. When training with data, the derivatives can either come from a pre-trained “forward KAN” or be found through finite differences or other methods.

Data \mathbf{X} relative noise	$\mathcal{K}(\mathbf{X})$ error	$\dot{\mathcal{K}}(\mathbf{X})$ error	Learned equation
0%	5.688e-08	–	$\frac{dx}{dt} = -0.0997x + 2.00044y$ $\frac{dy}{dt} = -2.00017x - 0.09963y$ $\frac{dz}{dt} = -0.29567z$
6.27%	1.255e-05	0.00014	$\frac{dx}{dt} = -0.10575x + 1.99087y$ $\frac{dy}{dt} = -2.00280x - 0.10184y$ $\frac{dz}{dt} = -0.26376z$
31.37%	0.00043	0.0101	$\frac{dx}{dt} = -0.12326x + 0.10216y^3 + 1.93752y + 0.0897z^3$ $\frac{dy}{dt} = -2.00878x - 0.12078y$ $\frac{dz}{dt} = -0.09579z^3 - 0.16220z$

Table 3: Relative errors and learned equations for the ODE case from section 4.2.1 with noise added to the training data. Errors are computed by the relative mean squared error (MSE).

B SINDy-KANs with noise

We consider the extension of SINDy-KANs to noisy data in this section using the test case from section 4.2.1. We progressively add more noise to the training data for \mathbf{X} , which increases the error in prediction of $\mathcal{K}(\mathbf{X})$. The accuracy of the learned equation depends directly on the derivative. To take the derivative, we first train a KAN to learn the map $\mathbf{x} \rightarrow \mathbf{X}$, denoted by $\mathcal{K}(\mathbf{X})$ (we call this the “forward KAN”). We then numerically take the derivative of the KAN prediction $\dot{\mathcal{K}}(\mathbf{X})$ using the autodifferentiation feature in JAX. An illustration of this process is given in Fig. 13.

We find that the SINDy-KANs are relatively robust up to 30% relative noise for this problem. At high noise level, higher order terms $((\cdot)^3)$ are erroneously learned, which could be alleviated by restricting the space of candidate functions for the SINDy-KANs. Alternatively, other methods for approximating the derivative $\dot{\mathbf{X}}$ could be used as have been successfully pursued in previous work with SINDy. Results for the case with the most noise are given in fig. 14.

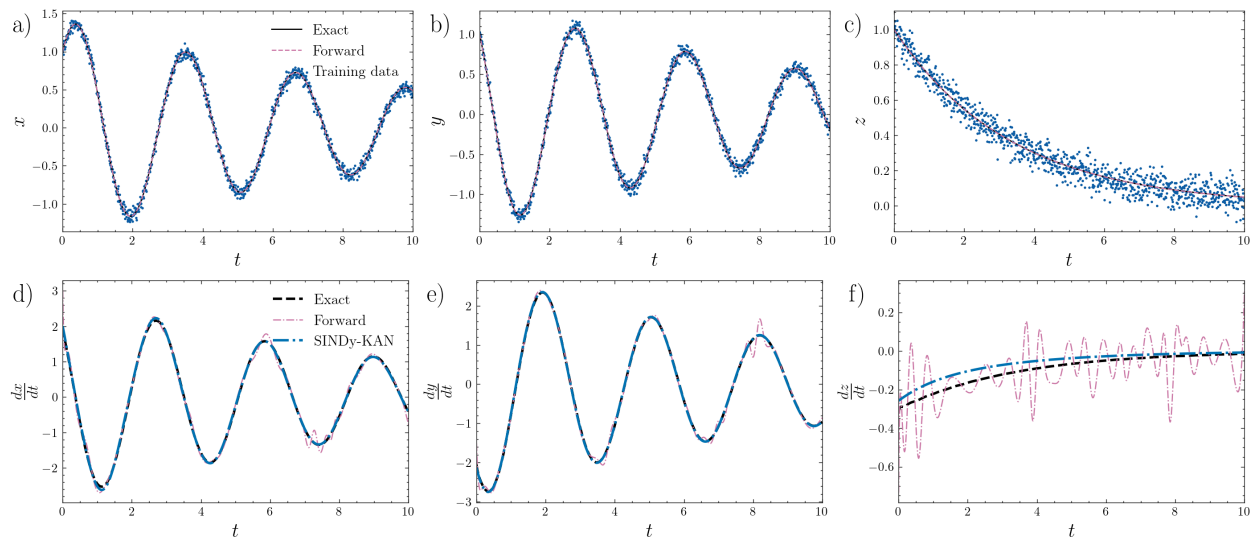


Figure 14: Results for the test case from section 4.2.1 with 31.37% relative noise added to the training data (a-c). Although the derivatives used to train the SINDy-KAN are noisy (d-f), the SINDy-KAN is able to recover most of the equation.

C Training parameters

Parameter	Sec. 4.1
KAN architecture	[2, 2, 1]
g	[3, 6]
Learning rate scales	[1, 0.6]
Boundaries	[0, 40k]
k	5
ADAM learning rate	1e-3
ADAM iterations	210k
λ_S	1
λ_Λ	1
λ_1	0.0001
λ_2	0.0001

Table 4: Hyperparameters used for training the results in section 4.1. g is the number of grid points used in the KANs. The grid is refined at the schedule denoted by the boundaries, and the learning rate is scaled at the same boundaries. k is the polynomial degree for the B-splines.

Parameter	Sec. 4.2.1	Sec. 4.2.2	Sec. 4.2.3	Sec. 4.2.4	Sec. 4.2.5
KAN architecture	[3, 3]	[2, 2]	[3, 6, 3]	[3, 5, 3]	[3, 6, 3]
g	[3]	[5, 10]	[5, 7]	[5, 7, 10]	[5, 7, 10, 15]
Learning rate scales	[1]	[1, .6]	[1, .6]	[1, .6, .6]	[1, .6, .6, .1]
Boundaries	[0]	[0, 50k]	[0, 30k]	[0, 30k, 60k]	[0, 30k, 60k, 300k]
k	5	5	5	5	5
ADAM learning rate	1e-3	1e-3	5e-3	5e-3	1e-2
ADAM iterations	20k	150k	50k	100k	500k
λ_S	1	1	10	10	0.1
λ_Λ	1	1	10	100	10
λ_1	0.0001	0.0001	0.001	0.001	0.0001
λ_2	0.001	0.001	0.001	0.001	0.0001

Table 5: Hyperparameters used for training the results in section 4.2. g is the number of grid points used. The grid is refined at the schedule denoted by the boundaries, and the learning rate is scaled at the same boundaries. k is the polynomial degree for the B-splines used.